Articles

Reduced Praseodymium Cluster Bromides Stabilized by Transition Metals

Rosa Llusar and John D. Corbett*

Department of Chemistry, Iowa State University, Ames, Iowa 50011

Received September 8, 1993®

Reactions of Pr turnings, $PrBr_3$, and metallic Z in Nb containers at 780–910 °C yield $Pr_6Br_{10}Z$ ($Y_6I_{10}Ru$ type) for Z = Co, Ru, Os, monoclinic Pr_3Br_3Ru (Pr_3I_3Ru type), and cubic Pr_3Br_3Z (Ca_3PI_3 type) for Z = Co, Os, Rh, Ir, Pt. Other Z elements investigated yield the binary Pr_2Br_5 or unknown phases. The structures of $Pr_6Br_{10}Co$ and $Pr_6Br_{10}Ru$ have been refined ($P\bar{1}$; $Z = 1$; $a = 9.359(4)$, $9.206(4)$ Å, $b = 9.243(5)$, $9.505(3)$ Å, $c = 7.538(3)$, $7.606(4)$ Å, $\alpha = 97.37(4)$, $97.08(4)°$, $\beta = 107.31(4)$, $107.47(4)°$, $\gamma = 110.17(3)$, $109.69(4)°$, $R = 4.3$, 5.2%, $R_w = 3.8$, 6.7%, respectively). The tetragonal compression in the 16-electron $Pr_6Br_{10}Ru$ (0.28 Å in d(Pr–Ru)) is notably greater than observed in the analogous $Y_6I_{10}Ru$, probably because of reduced matrix effects (repulsions) between the smaller bromide components. Earlier theoretical predictions regarding a one-over-two splitting of the parent t_{1u}^4 in the idealized octahedral iodide are therefore supported. The 17-electron $Pr_6Br_{10}Co$ shows a possibly related compression of 0.12 Å.

Introduction

The value of exploratory synthesis in solid-state chemistry has been manifested by the discovery of a great many new compounds, reactions, and structures that could not have been predicted on the basis of prior knowledge and understanding. The forecast of phase stability even among a collection of clear alternatives remains one of the great challenges in solid-state science, while the undiscovered possibilities sometimes seem to present almost insurmountable barriers.

The basic building block in cluster halides of the early transition and rare-earth metals is the M_6X_{12} unit in which halide atoms (X) bridge all edges of a nominal metal octahedron. These cluster units are found both isolated, with bridging halide interactions among them, and condensed into oligomeric, chain or network structures through shared metal atoms. The recognition that the very large number of cluster halide phases formed by group 3 and 4 metals are stable only when another interstitial element is included has led to a remarkable and diverse chemistry.[1-3]

To date, a variety of rare-earth-metal iodide structures have been reported in which the clusters are centered by transition metals.[4-12] On the other hand, neither the corresponding chlorides or bromides have exhibited anywhere near the variety of analogous cluster phases that has been seen with iodides, in part because the bromides have been less well studied. Even so, recent investigations by Dorhout and Corbett on the R–Br–Z systems for R = Y, Er led to the discovery of a remarkable R_4Br_4Os phase that contains confacial square antiprismatic chains of R centered by Os, a structural arrangement that is unprecedented among rare-earth-metal chloride or iodide systems.[13] Several studies have given clear evidence that the products formed are dependent on the size of both the host metal and the halogen.

In the present investigation, we have explored the stabilization of praseodymium bromide cluster phases through encapsulation of a variety of transition metal atoms. Among these, Co, Ru, Rh, Os, Ir, and Pt have led to the synthesis and characterization of new compounds in a variety of structure types, namely, triclinic $Pr_6Br_{10}Z$, monoclinic Pr_3Br_3Ru, and cubic Pr_3Br_3Z as well as to the recognition of other phases that are at present uncharacterized. The crystal structures of two of these compounds, $Pr_6Br_{10}Co$ and $Pr_6Br_{10}Ru$, have also been refined for comparison with the iodide analogues in which some very unusual dimensional variations with Z were seen earlier.[5,6]

Experimerntal Section

Materials. All compounds were manipulated under a dry nitrogen or argon atmosphere. The reactants in the form of Pr turnings (Ames Laboratory), sublimed $PrBr_3$, and the corresponding interstitial as high-purity metal, typically on a scale of ~200 mg, were welded in $^3/_8$ in. diameter niobium tubes prior to reaction. The elements Cr, Mn, Fe, Co, Ru, Rh, Pd, Re, Os, Ir, and Pt were investigated as potential Z. All of these were reacted as powders except for Co and Mn which were used as small pieces. The origin and purity of the elemental starting materials, the high-temperature synthetic techniques, and the Guinier powder X-ray diffraction methods have been described earlier.[6,14] In the following instances, phases of known structure type were identified by careful comparison of experimental patterns with those calculated on the basis of known parameters and space groups. Yields were estimated on the basis of the relative intensities of reflections from each component; only in critical instances were relative line multiplicities and cell contents also considered. Lattice constants were derived by least-squares refinement of indexed 2θ data.

Syntheses. $Pr_6Br_{10}Co$ was obtained in modest yields (ca. 30%) after reactions of compositions ranging from $Pr_6Br_{10}Co$ to Pr_3Br_3Co for 3

* Abstract published in *Advance ACS Abstracts,* February 1, 1994.

(1) Corbett, J. D.; Garcia, E.; Kwon, Y.-U.; Guloy, A. *Pure Appl. Chem.* **1990**, *62*, 103.
(2) Corbett, J. D. In *Modern Perspectives in Inorganic Crystal Chemistry*; Parthé, E., Ed.; NATO ASI Series C; Kluwer Academic Publishers: Dordrecht, The Netherlands, 1992, pp 27–56.
(3) Simon, A.; Mattausch, H. J.; Miller, G. J.; Bauhofer, W. *Handbook on the Physics and Chemistry of Rare-Earths*; 1991, Vol. 15, p 191.
(4) Hughbanks, T.; Corbett, J. D. *Inorg. Chem.* **1988**, *27*, 2022.
(5) Hughbanks, T.; Corbett, J. D. *Inorg. Chem.* **1989**, *28*, 631.
(6) Payne, M. W.; Corbett, J. D. *Inorg. Chem.* **1990**, *29*, 2246.
(7) Payne, M. W.; Dorhout, P. K.; Corbett, J. D. *Inorg. Chem.* **1991**, *30*, 1467.
(8) Payne, M. W.; Ebihara, M.; Corbett, J. D. *Angew. Chem., Int. Ed. Engl.* **1991**, *30*, 856.
(9) Dorhout, P. K.; Payne, M. W.; Corbett, J. D. *Inorg. Chem.* **1991**, *30*, 4960.
(10) Payne, M. W.; Dorhout, P. K.; Kim, S.-J.; Hughbanks, T.; Corbett, J. D. *Inorg. Chem.* **1992**, *31*, 1389.
(11) Ebihara, M.; Martin, J. D.; Corbett, J. D. *Inorg. Chem.*, submitted for publication.
(12) Park, Y.; Corbett, J. D. *Inorg. Chem.*, in press.
(13) Dorhout, P. W.; Corbett, J. D. *J. Am. Chem. Soc.* **1992**, *114*, 1697.
(14) Corbett, J. D. *Inorg. Synth.* **1983**, *22*, 15, 31.

0020-1669/94/1333-0849$04.50/0

Table 1. Lattice Constants (Å, deg) of $Pr_6Br_{10}Z$ and Pr_3Br_3Z Phases[a,b]

compd	no. of lines	*a*	*b*	*c*	α	β	γ
$Pr_6Br_{10}Co$	*c*	9.359(4)	9.243(5)	7.538(3)	97.37(4)	107.31(4)	110.17(3)
$Pr_6Br_{10}Ru$	31	9.206(4)	9.505(3)	7.606(4)	97.08(4)	107.47(4)	109.69(4)
$Pr_6Br_{10}Os$	34	9.272(2)	9.486(3)	7.614(2)	97.09(2)	107.48(2)	109.83(2)
Pr_3Br_3Co	14	11.833(1)			90	90	90
Pr_3Br_3Ru	15	8.884(2)	4.1872(9)	11.785(4)	90	94.62(2)	90
Pr_3Br_3Os	11	11.970(2)			90	90	90
Pr_3Br_3Rh	16	11.909(1)			90	90	90
Pr_3Br_3Ir	12	11.933(2)			90	90	90
Pr_3Br_3Pt	13	11.992(3)			90	90	90

[a] $Pr_6Br_{10}Z$: triclinic, $P\bar{1}$. Pr_3Br_3Z: cubic except Pr_3Br_3Ru, monoclinic. [b] λ = 1.540 562 Å. [c] Single-crystal diffractometer data (Mo Kα).

weeks at 850 °C. Cubic Pr_3Br_3Co (~10%) and an unknown phase were also present. $Pr_6Br_{10}Ru$ was synthesized in yields greater than 80% from stoichiometric reactions at temperatures between 780 and 900 °C. Once this phase has been formed, an increase of temperature to 1000 °C for 24 h followed by air quenching results in its decomposition and a 70% yield of the starting material, $PrBr_3$, plus an unknown phase that is not one of the known binary intermetallic compounds. $Pr_6Br_{10}Os$ has been prepared in yields higher than 80% from stoichiometric reactions run at ca. 825 °C for 2–3 weeks. Additional Pr does not yield another product.

Cubic Pr_3Br_3Co was obtained in ca. 50% yields from stoichiometric reactions at temperatures close to 850 °C for 3 weeks. About 30% $Pr_6Br_{10}Co$ and unknown material make up the balance. The isostructural Pr_3Br_3Rh and Pr_3Br_3Ir were prepared in >80% yields from stoichiometric reactions run at 850 or 910 °C for 3 weeks. When the Br:Pr ratio is increased to that corresponding to $Pr_6Br_{10}Z$, the yields go down to 40% and 10%, respectively, and in each case, isostructural new phases emerge in yields of ca. 40% and 80%, respectively. In the case of Rh, a third competing phase is also present. The isostructural Pr_3Br_3Os was obtained in good yields (>80%) from a reaction loaded for such a composition and run at 900 °C for 3–4 weeks. Pr_3Br_3Ru (monoclinic) was synthesized in ca. 90% yield from stoichiometric reactions at temperatures close to 900 °C for 3–4 weeks.

Reactions of Pr and $PrBr_3$ with Fe resulted in the identification of three new, unknown phases. Compositions investigated ranged over $1 \leq Br:Pr < 1.67$ and temperatures of 820–910 °C. In most cases, the binary phase Pr_2Br_5[15] was the major product (>60%). The erratic yields with which these new compounds were obtained suggest that the processes may be temperature as well as time dependent. Analogous reactions run with Cr, Mn, Re, or Pd at 850 °C for 3 weeks over a similar range yielded mostly Pr_2Br_5 (>70%), with a new phase also appearing with Mn. When Pt was used, cubic Pr_3Br_3Pt and another new phase were obtained; the latter remains unidentified.

Lattice constants for all of the new assigned phases are listed in Table 1.[16] Unless otherwise stated, these were all determined by Guinier techniques and referenced to NIST (NBS) Si powder as an internal standard.

X-ray Studies. Single crystals of $Pr_6Br_{10}Co$ and $Pr_6Br_{10}Ru$ suitable for X-ray diffraction experiments were obtained from reactions loaded as Pr_3Br_3Co and Pr_6Br_9Ru that had been run at 850 and 820 °C for 22 and 17 days and cooled slowly and quenched, respectively. The black crystals were sealed inside thin-walled capillaries under a nitrogen atmosphere, and hemispheres of data were collected on Rigaku AF6R and CAD4 diffractometers at room temperature to 50 and 60° in 2θ, respectively. Empirical absorption corrections (ψ scans) were utilized. Programs used were those in the instrument package TEXSAN.[17]

The structure of $Pr_6Br_{10}Co$ was solved using direct methods (SHELXS).[18] The least-squares refinement proceeded uneventfully and converged at $R, R_w = 4.3, 3.8\%$. The final difference Fourier map showed maximum and minimum peaks of 1.79 and −1.84 e/Å^3, respectively, the former being 1.23 Å from Pr1. The $Pr_6Br_{10}Ru$ refinement started with parameters for $Y_6I_{10}Ru$[5] and proceeded normally. DIFABS[19] was applied at the stage when $R, R_w = 5.9, 7.5\%$ since the absorption coefficient was quite large (301 cm^{-1}), and the refinement then converged at $R, R_w =$ 5.2, 6.7%. The larger Ru crystal and diffraction data from higher angles resulted in somewhat higher residuals but smaller ellipsoids and reduced errors in positional and thermal parameters and in distances than were secured for $Pr_6Br_{10}Co$. In both cases, the ellipsoid components for the Br1, Br2, Br3 atoms were elongated (ca. 2:1:1) along the $\bar{b}$, $\bar{a}$ and $\bar{c}$ directions, respectively. This effect has been observed before[5,6] and is characteristic of the anisotropic environments of these atoms.

Table 2. Selected Data Collection and Refinement Parameters for $Pr_6Br_{10}Z$

	$Pr_6Br_{10}Co$	$Pr_6Br_{10}Ru$
space group, Z[a]	$P\bar{1}$, 1	$P\bar{1}$, 1
no. of obs refls $[F_o^2 > 3\sigma(F_o^2)]$; variables	1095; 80	2690;80
μ(Mo Kα), cm^{-1}	308.8	301.3
transm factor range	0.462–1.00	0.803–1.266
R,[b] %	4.3	5.2
R_w,[c] %	3.8	6.7

[a] Dimensional data in Table 1. [b] $R = \sum||F_o|-|F_c||/\sum|F_o|$. [c] $R_w = [\sum w(|F_o| - |F_c|)^2/\sum w(F_o)^2]^{1/2}$; $w = \sigma_F^{-2}$.

Table 3. Positional and Isotropic Equivalent Displacement Parameters for $Pr_6Br_{10}Z$ (Z = Co, Ru)

atom	*x*	*y*	*z*	B_{eq},[a] Å^2
Pr1	0.0445(2)	−0.2432(2)	0.1249(2)	1.38(6)
Pr2	0.3089(2)	0.1049(2)	−0.0196(2)	1.51(6)
Pr3	0.1482(2)	0.1940(2)	0.3746(2)	1.43(6)
Br1	0.4770(4)	0.2830(6)	0.3789(6)	3.1(1)
Br2	0.0837(5)	0.4652(5)	0.2619(6)	2.7(1)
Br3	0.3680(4)	−0.1739(5)	0.0890(6)	2.7(1)
Br4	−0.1774(4)	0.0809(5)	0.4468(4)	1.7(1)
Br5	0.2715(4)	0.3679(4)	−0.1923(5)	1.7(1)
Co	0	0	0	1.1(2)
Pr1	0.05138(7)	−0.25344(7)	0.13594(9)	1.03(1)
Pr2	0.29263(7)	0.09191(7)	−0.02222(9)	1.06(1)
Pr3	0.1576(7)	0.19634(7)	0.38362(8)	1.09(1)
Br1	0.4813(2)	0.2820(2)	0.3711(2)	2.79(4)
Br2	0.0841(2)	0.4575(1)	0.2588(2)	2.57(4)
Br3	0.3725(1)	−0.1742(2)	0.0910(2)	2.44(4)
Br4	−0.1772(1)	0.0815(1)	0.4434(2)	1.31(3)
Br5	0.2709(1)	0.3606(1)	−0.1898(2)	1.41(3)
Ru	0	0	0	0.73(3)

[a] $B_{eq} = (8\pi^2/3)\sum_i\sum_j U_{ij}a_i^*a_j^*\bar{a}_i\bar{a}_j$.

Some relevant crystal and refinement data are given in Table 2, while atomic positions and isotropic-equivalent thermal parameters are listed in Table 3. More detailed information on the data collections and refinements as well as the anisotropic atom displacement parameters for both phases are present in the supplementary material. Structure factor data are available from J.D.C.

Results and Discussion

Syntheses. This investigation demonstrates that the stabilization of rare-earth-metal halide clusters by transition metal elements is neither restricted to or a copy of the iodide products. The first success in extending this chemistry to bromides afforded the phases R_4Br_4Os (R = Y, Er),[13] which have no known analogue

(15) Schleid, Th.; Meyer, G. *Z. Anorg. Allg. Chem.* **1987**, *552*, 97.
(16) Lattice constants tabulated earlier[6] for some $R_6I_{10}Z$ phases were incorrectly ordered *c*, *a*, *b*, γ, α, β.
(17) TEXSAN, version 6.0 package, Molecular Structure Corp., The Woodlands, TX (1990).
(18) Sheldrick, G. M. SHELXS-86. Institut für Anorgische Chemie, Universität Göttingen, Germany.
(19) Walker, N.; Stuart, D. *Acta Crystallogr.* **1983**, *A39*, 158.

in iodide chemistry.[20] In these cases, there are no near-lying competing cluster phases, and the compounds were obtained over a good range of temperatures and reaction stoichiometries, while inclusion of other potential interstitial atoms led either to no reaction or to other structures. When praseodymium is used as the host metal, the situation is quite different. In this case, no obvious Pr_4Br_4Z analogues are found, and the starting compositions, reaction temperatures, or both seem to have marked influences on the final product distributions. This behavior has a parallel in certain reduced rare-earth-metal iodide systems.[7,9]

Explorations with diverse transition metals as interstitials in praseodymium bromides have produced three triclinic $Pr_6Br_{10}Z$ phases for Z = Co, Ru, and Os, the monoclinic Pr_3Br_3Ru, and five cubic Pr_3Br_3Z examples for Z = Co, Rh, Os, Ir, and Pt (Table 1). The triclinic phases are isostructural with $Y_6I_{10}Ru$[5] while the monoclinic and cubic phases are members of the Pr_3I_3Ru[10] and Ca_3PI_3[21] (Gd_3Cl_3C[22]) families, respectively, and both involve cluster condensation via shared metal edges. The three $Pr_6Br_{10}Z$ examples can each be obtained under a particular set of conditions, sometimes over a range of compositions or temperatures (see Experimental Section). Each system also contains another cluster product; higher temperatures afford good yields of the cubic Pr_3Br_3Os and monoclinic Pr_3Br_3Ru phases while only mixtures of $Pr_6Br_{10}Co$ and cubic Pr_3Br_3Co were obtained over a range of compositions.

Under these conditions, there is no evidence of any bromide equivalent of the many rhombohedral $Pr_7I_{12}Z$ ($\simeq Pr^{3+}Pr_6I_{12}Z^{3-}$) members. The latter exist for Z = Cu, Ru, Rh, Pd, Re, Os, Ir, and Pt while only one triclinic product, $Pr_6I_{10}Os$, is found in the same systems.[6] Other rare-earth elements show different distributions between these two structure types.

All three group 9 metals Co, Rh, Ir stabilize cubic phases Pr_3Br_3Z. As the halogen:metal ratios are increased, the yields of these decrease, and new uncharacterized phases emerge for Rh and Ir. With Co, $Pr_6Br_{10}Co$ is the major competing phase. To date, the only praseodymium iodides of any kind that encapsulate group 9 metals are $Pr_7I_{12}Rh$, $Pr_7I_{12}Ir$, the condensed Pr_4I_5Co, and Pr_3I_3Ir (cubic).[6,8,9] Stable Pr_3I_3Z analogues appear to be limited to the three heaviest platinum metals. It is noteworthy that the high stability known for binary compounds that contain both an early, electron-poorer and a later, electron-richer transition metal[23] does not preclude the formation of these ternary compounds.

The present investigation also gave no glimpse of monoclinic phases isostructural with the condensed chain Pr_4I_5Z (Z = Co, Ru, Os).[7,20] The use of temperatures somewhat higher than normal (ca. 950 °C) that led to Pr_4I_5Ru gave monoclinic Pr_3Br_3Ru instead. Surprisingly, the cluster phase $Pr_6Br_{10}Ru$ decomposed to $PrBr_3$ when heated to ~1000 °C for short periods of time, in contrast with the fact that temperatures as high as 1020 °C afforded R_4Br_4Os as a single product. The stability of the latter, especially the seemingly important interchain bridge bonding, must depend critically on size proportions. Subtle differences among stabilities of sometimes several alternates that depend outwardly on the size and identity of the interstitial element as well as on the host metal and halogen are evident in these exploratory studies.

Structures and Bonding in $Pr_6Br_{10}Z$. An illustration of two clusters in the chain portion of the $Pr_6Br_{10}Ru$ structure is given in Figure 1. The characteristic Br4 atoms that bridge edges in two adjoining clusters (Br^{i-i}) are the means by which the stoichiometry is reduced below the classical M_6X_{12} type. These bridges occur in parallel with a pair of the more conventional $Br5^{i-a}$ (and the complementary $Br5^{a-i}$) functionalities, all four surrounding an inversion center. (The clusters are also centrosymmetric.) This construction continues left and right along $\vec{c}$ to generate quasi-infinite chains. Interchain bridging of the more common Br^{i-a} type provides the essential bonding at the other Pr1 and Pr2 vertices via Br2 and Br3 and generates the rest of the structural array along $\vec{b}$ and $\vec{a}$, respectively, as shown in Figure 2. These bridges are also centrosymmetric. The remaining $Br1^i$ is monofunctional. The more anisotropic environment about the last three types of bromine leads to the distinctive elongation of their thermal ellipsoids normal to the Pr–Br bonds. The cluster interconnections and compositions can be abbreviated as $Pr_6(Z)Br_2{}^iBr^{i-i}{}_{4/2}Br^{i-a}{}_{6/2}Br^{a-i}{}_{6/2}$.

Eighteen skeletal electrons appear to be optimal for nominally octahedral 6–12 type clusters that are centered by interstitials on which d orbitals are valence-active.[24] The first example of this structure, $Y_6I_{10}Ru$, was noteworthy in that it exhibited a marked tetragonal compression of the 16-electron cluster normal to the

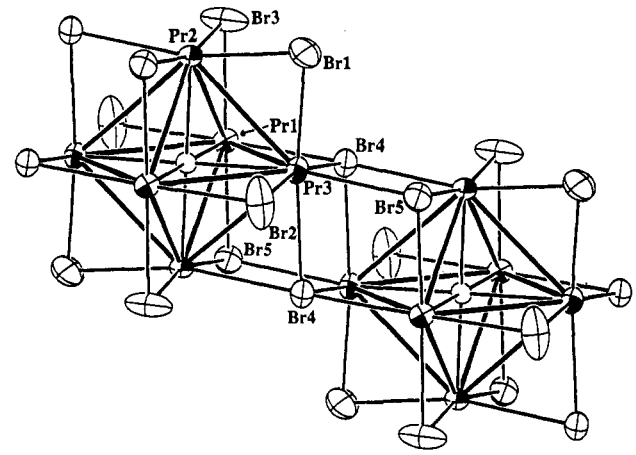

Figure 1. Representation of a pair of clusters in $Pr_6Br_{10}Ru$ showing the mode of $Br4^{i-i}$ and $Br5^{i-a}$ bridging between them. Such connections continue both left and right to generate infinite chains. The interstitial Ru lies on a center of symmetry (90% thermal ellipsoids).

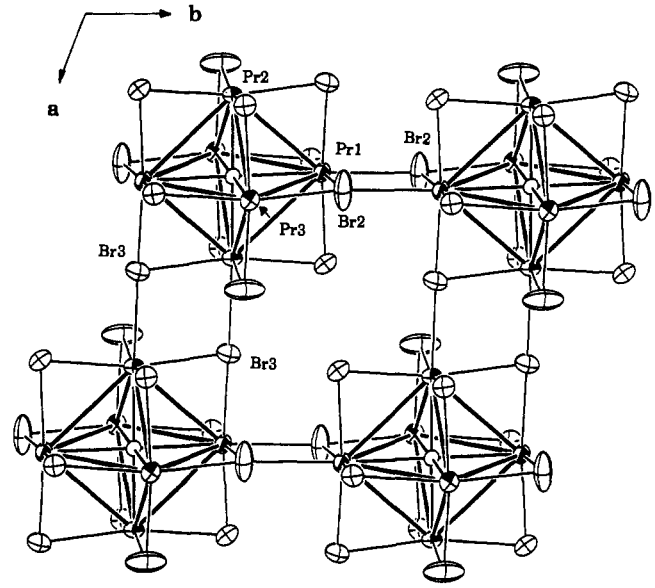

Figure 2. The centric pairs of Br^{i-a} bridges between cluster chains, approximately normal to Figure 1.

(20) However, phases of the R_4I_4Z stoichiometry that apparently contain confacial, centered antiprisms have also been found for R_4I_4Z (R = Sc, Y, Gd, Er; Z = Fe, Ru, Os, Ir, etc.), but these lack the valuable interchain halogen bridges present in R_4Br_4Os, and the structures can be refined only with R atoms that are very elongated along the chain axis. The problem appears to be intrinsic; no diffraction evidence for incommensurability has been found: Lachgar, A.; Ebihara, M.; Park, Y.; Dorhout, P. K.; Corbett, J. D. Unpublished research.

(21) Hamon, C.; Marchiand, R.; Laurent, Y.; Lang, J. *Bull. Soc. Fr. Miner. Crist.* **1974**, *97*, 6.

(22) Warkentin, E.; Simon, A. *Rev. Chim. Miner.* **1983**, *20*, 488.

(23) Brewer, L.; Wengert, P. R. *Met. Trans.* **1973**, *4*, 83.

(24) Hughbanks, T.; Rosenthal, G.; Corbett, J. D. *J. Am. Chem. Soc.* **1986**, *108*, 8289.

Table 4. Important Distances (Å) and Angles (deg) in $Pr_6Br_{10}Co$ and $Pr_6Br_{10}Ru$

distance	$Pr_6Br_{10}Co$	$Pr_6Br_{10}Ru$	distance	$Pr_6Br_{10}Co$	$Pr_6Br_{10}Ru$
Pr1–Pr2	3.831(3)	3.850(2)	Pr2–Br1	2.888(5)	2.943(3)
Pr1–Pr2[a]	3.849(3)	3.885(2)	Pr2–Br3	2.978(5)	3.016(2)
Pr1–Pr3	3.883(4)	4.108(2)	Pr2–Br3[b]	3.086(4)	3.135(2)
Pr1–Pr3[a]	3.821(3)	4.035(2)	Pr2–Br4	3.099(4)	3.096(2)
Pr2–Pr3	3.828(3)	3.800(2)	Pr2–Br5	2.976(5)	3.030(2)
Pr2–Pr3[a]	4.030(2)	3.987(3)			
Pr1–Z	2.659(2)	2.861(1)	Pr3–Br1	2.887(4)	2.847(2)
Pr2–Z	2.771(2)	2.603(1)	Pr3–Br2	2.941(5)	2.974(2)
Pr3–Z	2.787(3)	2.897(2)	Pr3–Br4	3.100(4)	3.098(2)
Pr1–Br2	2.972(5)	3.003(3)	Pr3–Br4	3.079(5)	3.126(2)
Pr1–Br2[b]	3.105(5)	3.088(2)	Pr3–Br5[b]	3.115(5)	3.111(2)
Pr1–Br3	2.974(4)	2.932(2)	Br1–Br2[c,d]	3.849(6)	3.861(4)
Pr1–Br4	3.050(4)	3.076(2)	Br3–Br4[d]	3.944(5)	3.900(4)
Pr1–Br5	3.004(4)	2.967(2)	Br4–Br5	3.968(5)	3.966(4)

angle	$Pr_6Br_{10}Co$	$Pr_6Br_{10}Ru$
Pr1–Z–Pr3	90.92(7)	91.02(5)
Pr1–Z–Pr2	90.27(6)	90.53(4)
Pr2–Z–Pr3	87.06(7)	87.24(6)
Br2–Pr1–Br4	167.2(1)	172.90(4)
Br3–Pr1–Br5	168.3(1)	174.60(4)
Br1–Pr2–Br4	171.8(1)	166.24(4)
Br3–Pr2–Br5	168.5(1)	165.47(4)
Br1–Pr3–Br4	168.4(1)	171.78(5)
Br2–Pr3–Br4	167.5(1)	167.32(5)
Z–Pr1–Br2	178.0(1)	175.92(3)
Z–Pr2–Br3	171.3(1)	173.69(4)
Z–Pr3–Br5	170.70(9)	168.83(3)
Pr1–Br4–Pr3	78.6(1)	82.95(5)
Pr1–Br4–Br3	99.0(1)	98.24(6)
Pr2–Br4–Pr3	81.10(9)	80.14(6)
Pr2–Br4–Pr3	97.4(1)	96.42(5)
Pr3–Br4–Pr3	99.2(1)	100.51(5)

[a] Inversion-related atom. [b] Exo Br^{a-i}. [c] Only Br–Br < 3.97 Å are listed. [d] Intercluster distances.

chain (Y2–Ru–Y2). Whether this was caused by the anisotropic cluster linkages or for reasons related to the electronic configuration was apparently settled in favor of the latter by extended-Hückel calculations. Interactions between 4d orbitals on Y cause a splitting of the nominal t_{1u}^4 HOMO into a counterintuitive, two-below-one pattern, largely because Ru 5p levels lie too high to be important in Y–Ru bonding.[5] However, this picture was muddied somewhat when a much smaller distortion was later found in the 16-electron $Y_6I_{10}Os$, and an even smaller one (in the R3 direction) in the 17-electron $Y_6I_{10}Ir$. Relativistic effects were imagined to be responsible in the Os case.[6] In order to extend this inquiry, we have refined the structures of $Pr_6Br_{10}Ru$ and $Pr_6Br_{10}Co$ in which there are 16 and 17 cluster-based electrons, respectively. These give both another Ru and a smaller 17-electron comparison in clusters where there are presumably smaller matrix effects, if any. Important bond distances and angles are listed in Table 4.

Bonding within the most important part of the structure, the cluster itself, is dominated by strong Pr–Z bonding, though the polar Pr–Br contributions are also significant. The first is emphasized in the cluster view shown in the Table of Contents. Notable differences between the two structures are again found in the Pr–Z distances. For comparison, these, together with the $Y_6I_{10}Z$ data, Z = Ru, Os, Ir, are collected in Table 5. The 16-electron $Pr_6Br_{10}Ru$ example shows an even greater axial compression than what first sparked our interest in $Y_6I_{10}Ru$. The R2–Ru compression of 0.206(5) Å (relative to the average of R1–Ru and R3–Ru) in $Y_6I_{10}Ru$ has now become 0.276(3) Å in $Pr_6Br_{10}Ru$. We infer that this arises from reduced matrix effects in the presence of both the larger Pr and, particularly, the smaller bromide, that is, from fewer restrictions on the cluster R–R, R–Ru, and R–X^a bond lengths brought on by closed-shell X···X contacts.[2]

Table 5. Cluster Distortions (Å) in $R_6I_{10}Z$ Phases

	cluster-electron count		
	16	16	17
compd	$Y_6I_{10}Ru$[a]	$Y_6I_{10}Os$[b]	$Y_6I_{10}Ir$[b]
Y1–Z	2.752(3)	2.7179(8)	2.6947(7)
Y2–Z	2.556(3)	2.6438(9)	2.6912(9)
Y3–Z	2.772(3)	2.750(1)	2.7283(8)
Δd [odd axis]	–0.206(5) [Y2]	–0.090(2) [Y2]	+0.035(1) [Y3]
$\bar{d}$	2.693	2.704	2.705
compd	$Pr_6Br_{10}Ru$		$Pr_6Br_{10}Co$
Pr1–Z	2.861(1)		2.659(2)
Pr2–Z	2.603(1)		2.771(2)
Pr3–Z	2.897(2)		2.787(2)
Δd [odd axis]	–0.276(3) [Pr2]		–0.120(3) [Pr1]
$\bar{d}$	2.787		2.739

[a] Reference 5. [b] Reference 6.

Note that the compression axes both in $Pr_6Br_{10}Z$ and for all but $Y_6I_{10}Ir$ are normal to the R3–Z chain axis (Figure 1) so that the unusual bonding mode along the latter does not seem to be involved. In fact, the R3–Z distances are generally only a few hundreths of an angstrom longer than along the other, "unaffected" axes (Figure 2).

The applicability/suitability of the earlier EHMO calculations and the resultant interpretation appear to be strengthened by the present results. Comparable calculations were done on the idealized D_{4h} $Pr_6(Ru)Br_{10}Br_8^{8-}$ cluster with exo bonding included, STO orbital exponents, and energies from charge-consistent studies on similar compounds.[5,7] Relativistic atomic orbital energies were taken for Pr. Again, the two-below-one pattern arises with the HOMO and LUMO orbitals having mainly Pr 5d character. The magnitude of the gap is similar (~0.3 eV) to that calculated for $Y_6Br_{10}Ru$, and it is mainly determined by the Pr–Pr interactions.

Pure samples of any ruthenide with diamagnetic cations have not been obtained to check these expectations magnetically. The 17-electron cobalt example shows an appropriately smaller (0.120(3) Å) Pr–Co compression but in the other direction (toward Pr1) that does not involve the chain condensation (Figure 1). The sole exception in proportions found earlier within $Y_6I_{10}Ir$ also may have been obscured by matrix or relativistic effects, or both. Single-crystal results for "normal" 18-electron $R_6X_{10}Z$ examples are not available.

A matrix effect in $Y_6I_{10}Ru$ was expected to be particularly important in the Y2–I3 distance that lies trans to the short Y2–Ru, and this was reflected in a 0.097(7) Å longer distance. This is reasonably reduced to 0.035(3) Å for the larger Pr and smaller Br; in fact, the distribution of all Pr–Br^{a-i} distances is now within a range of only 0.05 Å. The difference in average Pr–Z distances in the two bromides, 0.05 Å with Ru larger, is in the "ballpark" of the difference in single-bond metallic radii, 0.08 Å.[25] The same applies to the average R–Ru distance difference for Pr vs Y. Average Pr–Br distances are consistently in the neighborhood of 0.01 Å larger for Ru than for Co. Variations in d(Pr–Br) with bromine function are as usual, $Br^i < Br^{i-a} < Br^{i-i} < Br^{a-i}$.

Pr_3Br_3Z Phases. Two different structure types are known with this stoichiometry. As with Pr_3I_3Ru, Pr_3Br_3Ru has only been prepared as the monoclinic version. Marked distortions in the iodide double-chain structure that could be easily discerned in the a/b lattice ratios[10] suggest Pr_3Br_3Ru will lie nearer the relatively undistorted iodide version. This presumes, however, that changes in X^{a-i} bridging along a will decrease that dimension with bromide about the same as the 0.09-Å reduction in b along the cluster condensation axis, which may be debatable.

The stabilization of cubic phases in a defect NaCl (Ca_3PI_3) structure with an identical stoichiometry occurs for Pr_3Br_3Z with

(25) Pauling, L. *The Nature of the Chemical Bond*; Cornell University Press: Ithaca, NY, 1960; p 400.

the interstitial elements Co, Rh, Ir, Os, and Pt. Iodide members are known for La and Pr with Os, Ir, and Pt, but not Rh or Ru (Co was not investigated). This investigation shows that lighter elements can also be incorporated by changing only the nature of the halide. Lattice parameters follow changes in metallic radii of Z down the group 9 elements; an increase of 0.076(1) Å in *a* between Co and Rh is followed by an increase of 0.024(2) Å between Rh and Ir. In contrast, the parameter changes between Os and Ir do not follow Z radii, which increase slightly over the series; instead, a 0.037(3) Å decrease is observed. The last decrease is much more pronounced for the iodide analogues, viz., 0.12(1) Å. It must be remembered that the lattice parameter changes reflect a composite of R–Z and R–X^a effects.

Another noteworthy observation from this investigation is the apparent existence of a remarkable number of previously undiscovered cluster structures, as evidenced by the sizable number of unknown powder patterns found. As far as we can tell, these are neither intermetallic (PrZ_x) side products nor other phases that are independent of the identity of Z.

Acknowledgment. This research was supported in part by the National Science Foundation, Solid State Chemistry, via Grants DMR-8902954 and -9207361, and was carried out in the facilities of Ames Laboratory, DOE. R.L. thanks NATO for Fellowship support.

Supplementary Material Available: Tables of data collection and refinement details and of anisotropic atom displacement parameters for $Pr_6Br_{10}Co$ and $Pr_6Br_{10}Ru$ (3 pages). Ordering information is given on any current masthead page.